Generalized Nonvolcanic Tremor Signal for Characterizing the Seismic Process of Great East Japan Earthquake

Hiroyuki Kikuchi[1]

[1]Seismic Lab

November 23, 2022

Abstract

The generalized nonvolcanic tremor has been proposed for characterizing the seismic process of megathrust earthquakes. A tremor signal with a vibrational velocity of microns per second exhibit the dominant frequency of 1 Hz to 10 Hz in the Fourier amplitude spectrum. Paying attention to the negative curvature of the spectrum, we generalize the tremor and define alpha-tremor as the degree of the negative curvature of the spectrum in the frequency range of 2.97 Hz to 9.80 Hz. Significant tremors and background vibrations are respectively represented by large positive alpha-tremors and non-positive alpha-tremors. Alpha-tremor is evaluated for ground vibration data acquired every 0.05 seconds for approximately 10 years at three seismic stations. At the station 188 km away from the epicenter of the Great East Japan Earthquake (GEJE) of magnitude 9, symmetries regarding the seismic process of the GEJE have been found. Among the observed 9 prominent peaks of the positive alpha-tremor, the first and last peak appears 3 years before and after GEJE, respectively. The frequency distributions of the alpha-tremor during 3 years before and after GEJE match by 99.95%. The statistical distribution that properly approximates the frequency distribution of the positive alpha-tremor is found to be the Gumbel distribution, rather than the Gaussian distribution. The time evolution of the frequency distribution of the alpha-tremor at the seismic station 1170 km away from the GEJE epicenter suggests that GEJE may have affected the ground motion there, and initiated the seismic process of the M7.3 earthquake that occurred near the station.

Generalized Nonvolcanic Tremor Signal for Characterizing the Seismic Process of Great East Japan Earthquake

Hiroyuki Kikuchi[1*]

[1]Seismic Lab, 307, 12-1, 2-Chome, Wakamiya, Okegawa-shi, Saitama 363-0022, Japan

Key Points:

- α-tremor is defined as the degree of the negative curvature of the Fourier spectrum in 2.97-9.80 Hz range
- α-tremor calculated from ground vibration data continuously evaluates ground activity during the silent period
- Seismic process of a megathrust earthquake can be statistically discussed by introducing α-tremor

*307, 12-1, 2-Chome, Wakamiya, Okegawa-shi, Saitama 363-0022, Japan

Corresponding author: Hiroyuki Kikuchi, hkikuchi@kkh.biglobe.ne.jp

Abstract

The generalized nonvolcanic tremor has been proposed for characterizing the seismic process of megathrust earthquakes. A tremor signal with a vibrational velocity of microns per second exhibit the dominant frequency of 1 Hz to 10 Hz in the Fourier amplitude spectrum. Paying attention to the negative curvature of the spectrum, we generalize the tremor and define α-tremor as the degree of the negative curvature of the spectrum in the frequency range of 2.97 Hz to 9.80 Hz. Significant tremors and background vibrations are respectively represented by large positive α-tremors and non-positive α-tremors. α-tremor is evaluated for ground vibration data acquired every 0.05 seconds for approximately 10 years at three seismic stations. At the station 188 km away from the epicenter of the Great East Japan Earthquake (GEJE) of magnitude 9, symmetries regarding the seismic process of the GEJE have been found. Among the observed 9 prominent peaks of the positive α-tremor, the first and last peak appears 3 years before and after GEJE, respectively. The frequency distributions of the α-tremor during 3 years before and after GEJE match by 99.95%. The statistical distribution that properly approximates the frequency distribution of the positive α-tremor is found to be the Gumbel distribution, rather than the Gaussian distribution. The time evolution of the frequency distribution of the α-tremor at the seismic station 1170 km away from the GEJE epicenter suggests that GEJE may have affected the ground motion there, and initiated the seismic process of the M7.3 earthquake that occurred near the station.

1 Introduction

Strong earthquakes are a major concern in disaster management, and various measures are being taken for strong earthquakes. Earthquake Early Warning system in Japan warns people when an earthquake of 5 or greater is expected on the Japan seismic scale. When an earthquake is detected, the system analyzes the data captured by seismographs near the epicenter to estimate the epicenter, the magnitude of the earthquake and the seismic intensity. The estimated information is quickly released so that people can move to safe places or evacuate from dangerous places before strong surface waves arrive. Regarding building regulations, the seismic standards of the Building Standard Law in Japan require minor damage in medium-scale earthquakes with a seismic intensity of 5 or greater, and no collapses in large-scale earthquakes with a seismic intensity of 6 to 7. On the other hand, earthquakes generally last less than a minute, and the dominant state of ground motion is seismically silent. Therefore, in order to understand the seismic process, it is necessary to investigate the silent state.

Nonvolcanic tremor is one of the notable discoveries regarding the silent state. Obara investigated the seismically silent period in southwest Japan and identified the nonvolcanic tremor, the weak but noticeable signal with typical frequency range of 1?10?Hz (Obara, 2002). Obara discussed that tremor with a long duration time is possibly caused by a chain reaction of small fractures induced by fluid. In 2003, tremors were related to ground slip events. Tremor activity accompanied by a slip event was observed approximately every 12 months for 6 consecutive years at Cascadia subduction zone interface (Rogers & Dragert, 2003). Regarding the mechanism of the long duration tremor, Peng and Chao observed the tremor induced by an earthquake and discussed that tremor occurred as a simple frictional response to the driving force (Peng & Chao, 2008).

In this study, nonvolcanic tremors are generalized in a way that represents not only tremors but also non-tremors, so the generalized tremors continuously characterize the ground motion before and after GEJE, Great East Japan Earthquake of magnitude 9. The rest of this paper is organized as follows: First, methods of the processing ground vibration data are explained. Second, tremors are observed. Third, the tremor is generalized. Finally, the generalized tremor is applied to the ground vibration data acquired at three seismic stations KSN, HID and TMC, which are respectively 188 km, 586 km and 1170 km away from the GEJE epicenter (Fig. 1). In this paper, time is Japan Standard Time.

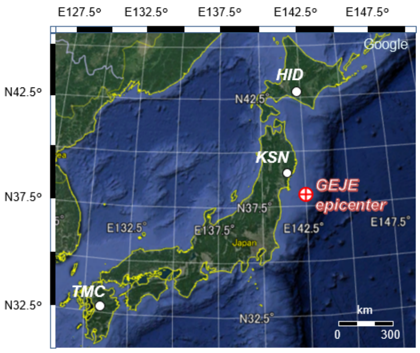

Figure 1: Seismic stations and epicenter of Great East Japan Earthquake (GEJE).

2 Observation of tremor signals

Ground vibration velocity data acquired every 0.05 seconds at the three seismic stations is downloaded in chronological order from the web site of F-net, broadband seismograph network of National Research Institute for Earth Science and Disaster Resilience (NIED, 2019). The data is converted to piecewise deviation. Each section consists of 10 velocity data, and the piecewise deviation is the difference between the velocity within the section and the average velocity within the section. The piecewise deviation fluctuates around zero, and its squared average is the dispersion in statistics. The piecewise deviation data is divided into blocks of 1024 data, which corresponds to the data acquisition time of 51 seconds, and the Fourier amplitude of each block is calculated. The Fast Fourier Transform (FFT) algorithm is applied with no overlap, and no filtering. The upper bound of the frequency domain is 10Hz, which is half the data acquisition frequency. The lower bound is 0.02 Hz which is determined by the block size 1024. Therefore, the FFT with the sampling frequency of 20Hz and the block size of 1024 is equivalent to an FFT with a 0.02-10 Hz bandpass filter.

Fig. 2 shows a comparison of the velocities and velocity spectrograms in the up-down (UD), north-south (NS), and east-west (EW) direction. The velocity data was acquired at KSN every 0.05 seconds from Mar. 3, 2011 to March 11, 2011. The period includes the magnitude 9 Great East Japan Earthquake (GEJE) occurred at 14:46 on March 11, 2011. The tremor signals are shown as the vertical brown lines in the 1 Hz to 10 Hz range of the spectrograms. In the quiet period before the earthquake of magnitude 7.3, the timing of the vertical brown lines in the spectrograms (Fig. 2 (a4), (b2), and (c2)) respectively matches the timing of the wave clusters which have larger amplitude than surroundings (Fig. (a3), (b1), and (c1)). Since the UD component contains greater number of tremor signals than the other components, we focus on the UD component in the later sections.

The third brown tremor line in Fig. 2 (a4), which corresponds to the velocity deviation in Zone_A in Fig. 2 (a3), constructs a finer spectrogram structure. Fig. 3 shows the details of the Zone_A of 12500 second duration. The velocity deviation and its spectrogram are shown in Fig. 3 (a) and 3 (b), respectively. Fourier amplitude spectrum and its 10 moving averages are respectively indicated by the black and red lines in the Log10-

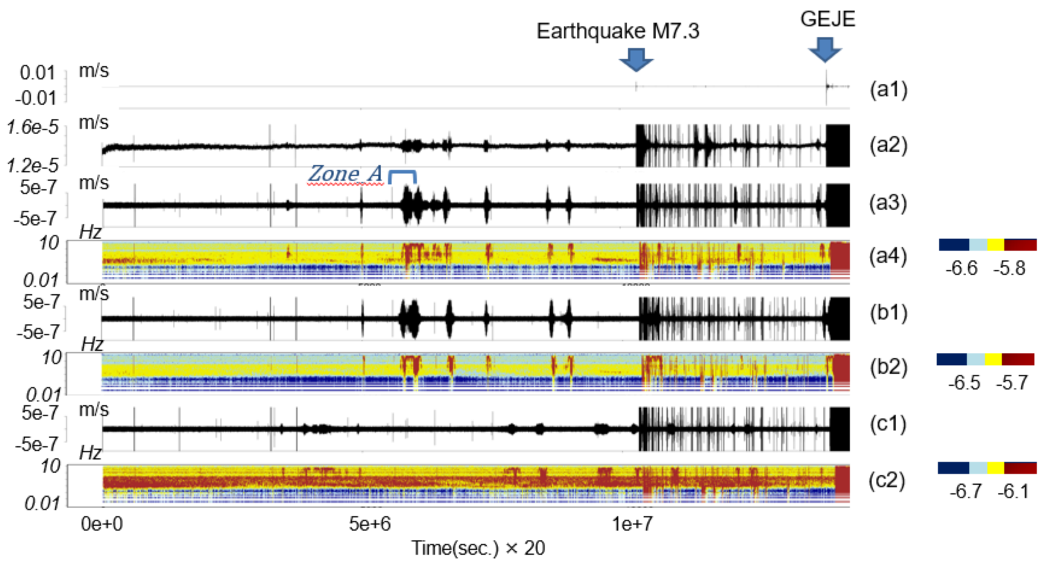

Figure 2: Tremor signals at KSN during March 3, 2011 to March 11,2011 period . (a1) Ground velocity (m/s) in UD direction. (a2) Magnified plot of (a1). (a3) Piecewise deviation of (a2). (a4) Spectrogram of (a3). (b1) Piecewise velocity deviation in NS direction. (b2) Spectrogram of (b1). (c1) Piecewise velocity deviation in EW direction.

Log10 plots of Fig. 3 (c1) to 3 (c6). The spectrogram is plotted from the 10 moving averages. The velocity deviations in Fig. 3 (d1) to 3 (d6) are the source data for the amplitude spectrum. The number below the velocity deviation graph indicates the time interval (seconds x 20). The velocity deviations are extracted from the beginning, center, end, and their intermediates of the period shown in Fig. 3 (a), and are chronologically exhibited from left to right. The first amplitude spectrum is non-tremor (Fig. 3 (c1)). The rest of the spectrums are tremor signals showing large value and negative curvature in 1-10Hz (Fig. 3 (c2) to 3 (c6)). The curvature widens at the center of the zone and sharpens at the beginning and end of the zone. Similarly, the velocity deviation amplitude is small at the start and end, and large at the center.

3 Definition of α-tremor

The curvature of the Fourier amplitude spectrum is defined as the ratio of $P_i - P_{ni}$ to $|P_2 - P_1|$ in Fig. 4 (a), where P_j is the point of the (frequency, spectrum) coordinate system. The frequency of P_1 and P_2 are 2.97 Hz and 9.8 Hz, which correspond to the 152th and 502th point on the frequency axis, respectively. The average of the spectrum value of the nearest 5 points are assigned as the spectrum value for the P_1 and P_2. P_i is a point in the 2.97-9.8 Hz range. P_{ni} is determined so that the line from P_i to P_{ni} is perpendicular to the line connecting P_1 and P_2. If the spectrum value of P_i is greater than that of P_{ni}, the curvature is positive. Otherwise, the curvature is non-positive. The curvature is independent of the scale change since the line length in log10 plot is invariant to the scalar multiplication of the coordinate values.

We define α-tremor as the curvature of which absolute value is greater than the absolute value of other curvatures in the frequency range of 2.97 to 9.8 Hz (Fig. 4 (a)). An arbitrary ground velocity signal is classified as either α-tremor or non-α-tremor. Pos-

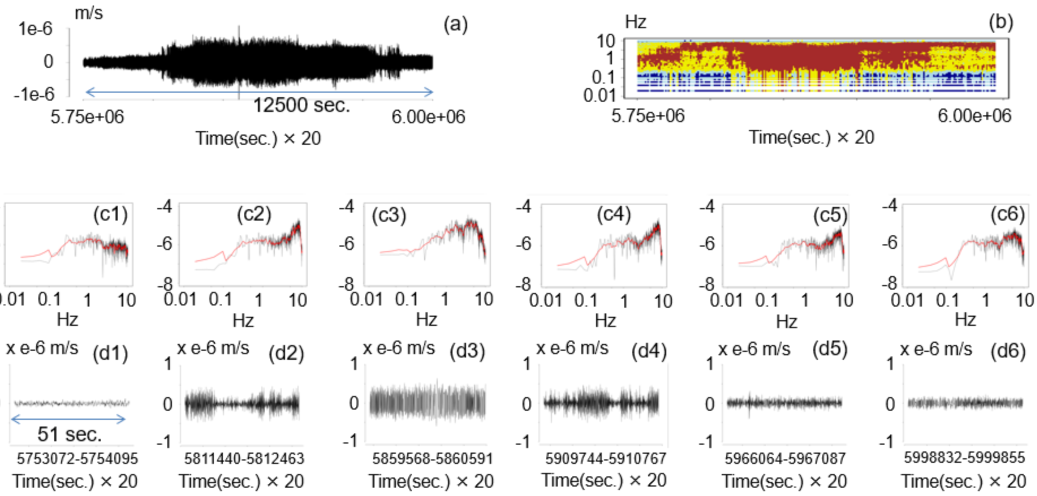

Figure 3: Fine structure of the tremor signal in the Zone_A in Figure 2 (a3). (a) UD velocity deviation (m/s). (b) Spectrogram of (a). (c1)-(c6) Fourier amplitude spectrum excerpted from (b). (d1)-(d6) UD velocity deviation, the source data for (c1)-(c6).

itive α-tremor includes the tremor, and non-positive α-tremor corresponds to non-tremor or background signals.

The α-tremor for the velocity data acquired at KSN during March 03, 2011 to March 11, 2011 is exhibited in Fig.4 (b). The positive peaks of the α-tremor are similar to the brown lines in Fig. 2 (a4) as expected.

It should be noted that the piecewise velocity deviation is equivalent to the raw velocity data in evaluating the α-tremor. Fig. 5 (a) compares the Fourier amplitude spectrum of the deviation data of a tremor signal to the amplitude spectrum of the raw velocity data. In the range of 2.97 Hz to 9.8 Hz, the amplitude spectrum of the deviation velocity (black line) matches the spectrum of the raw data (green line) by 80%. Therefore, we may select either the piecewise deviation velocity data or the raw velocity data to obtain a unique amplitude spectrum in the range 2.97 Hz to 9.8 Hz. The α-tremor in the subsequent sections is calculated from the raw velocity data for convenience. The orange and red lines in Fig. 5 (a) are the 10 moving averages of the black and green lines, respectively. The source data of the spectrum, which are the velocity deviation and velocity acquired at KSN during the period from March 1, 2012 to March 10, 2012, are shown in Fig. 5 (b) and 5 (c), respectively.

4 Ground motion characterization by α-tremor

The α-tremor is evaluated for the data acquired at KSN, HID, and TMC every 0.05 seconds for over 10 years. The results are discussed in the subsections containing the figures which include tables, maps and plots. In the table, the ID is the identifier of an earthquake, and the latitude, longitude and depth indicate the location of the epicenter. The table includes date, magnitude, and seismic intensity of earthquakes searched on the website of the Japan Meteorological Agency of Ministry of Land, Infrastructure, Transport and Tourism (JMA-1, 2019). The search conditions are the seismic intensity greater than 4, the location of observing the seismic intensity, and the time period specified in each subsection. The observation point of the seismic intensity is marked with a filled blue

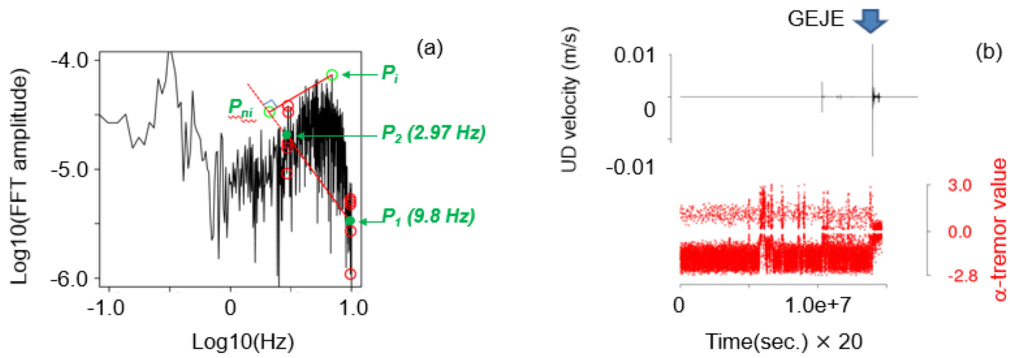

$$Curvature\_i \equiv \frac{P_i - P_{ni}}{|P_2 - P_1|} \;;\; 2.97\,Hz < f_i(frequency) < 9.8\,Hz$$

$$\alpha\text{-}tremor \equiv Curvature\_m \,;\; |Curvature\_m| = \max(|Curvature\_i|)$$

Figure 4: Definition of α-tremor. (a) Definition of spectrum curvature and α-tremor. (b) α-tremor calculated for the UD velocity data of $Fig.2(a1)$.

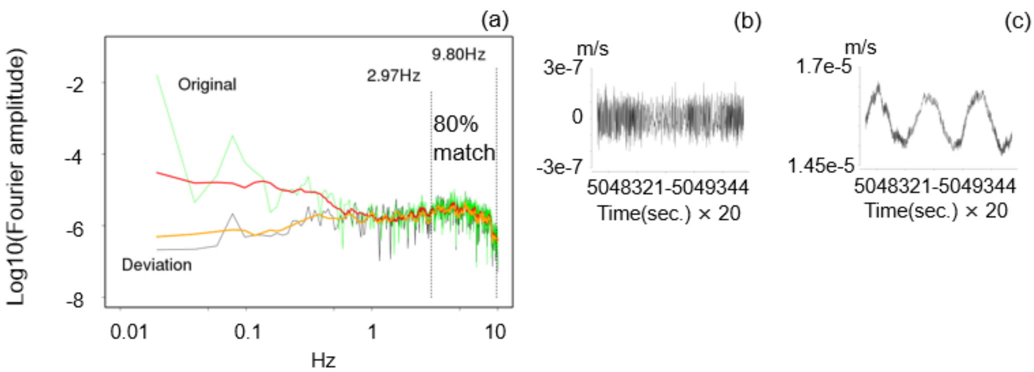

Figure 5: Comparison of velocity deviation and velocity. Tremor signal recorded at KSN from March 1, 2012 to March 10, 2012. (a) Fourier amplitude spectrum of velocity in the UD direction and its deviation velocity. (b) UD velocity deviation data. (c) UD velocity data.

rectangle on the map. The white circle and red $\oplus$ on the map are the location of the seismic station and the epicenter of the earthquake, respectively. The plot contains the positive α-tremor in log10 format, and the timing of earthquakes with seismic intensities greater than 4 as indicated by the red up arrow and earthquake ID. In this paper, the seismic intensity is described using the seismic intensity class of the Japan Meteorological Agency. The seismic intensity of 4 corresponds to the intensity that most people are frighten when they experience it.

4.1 KSN

Fig. 6 shows the positive α-tremor observed at KSN from Jan. 1, 2006 to Dec. 30, 2018, and the timing of earthquakes with seismic intensities greater than 4. For GEJE of magnitude 9, seismic intensity 6 was recorded at Kesennuma City, which is the observation point of seismic intensity approximately 10km from KSN. Several α-tremor peaks are observed at KSN before and after GEJE. Since the timing of the α-tremor peaks do not match the timing of the earthquakes A and D, those α-tremors are probably not induced by earthquakes.

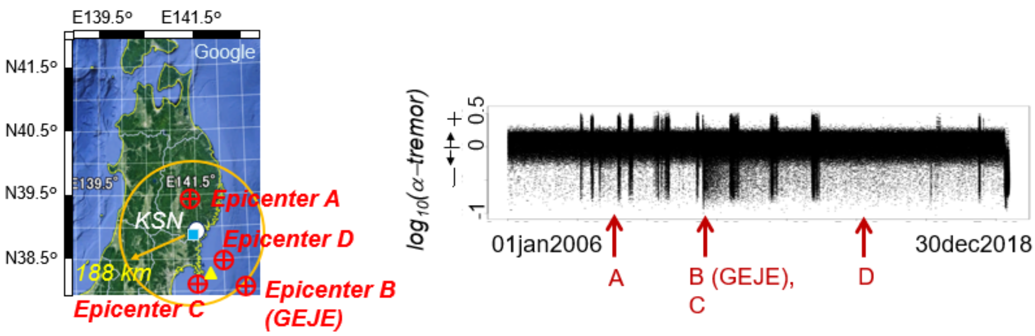

ID	Date	Magnitude	Seismic Intensity	Latitude	Longitude	Depth(km)
A	Jul. 24, 2008	6.8	5	$39.43N$	$141.38E$	108
B	Mar. 11, 2011	9	6	$38.06N$	$142.51E$	24
C	Apr. 07, 2011	7.2	5	$38.12N$	$141.55E$	66
D	May 13, 2015	6.8	5	$38.52N$	$142.09E$	46

Figure 6: Positive α-tremor at KSN from January 1, 2006 to December 30, 2018.

Exactly 3 years of α-tremor before and after GEJE have been extracted and shown in Fig. 7 (a) along with the index of α-tremor peaks. The index is underlined for peaks after GEJE. Fig. 7 (b) shows the time duration of the peaks, and the duration of the intervals between the peaks. The bars filled in red and yellow are the time duration of the peak and the duration between the peak and the previous peak, respectively. The peak and interval durations are respectively 0.6 to 4.3 months and 2.4 to 9.4 months. The duration between the two peaks tends to be longer after GEJE. On the other hand, there is symmetry with respect to GEJE. Fig. 7 (c) compares the frequency distribution of the α-tremor before GEJE to that after GEJE. They are 99.95% matched in evaluating Pearson's correlation coefficient. The argument on the symmetry, as well as the discussions on the mechanism of the initiation and termination of the α-tremor peak respectively before and after GEJE, are left for the further study.

The α-tremor peak constructs the fine structure of 33 micropeaks, as shown in Fig. 8 (a), which is an enlarged view of the peak No.4 in Fig. 7 (a). Fig. 8 (b1) shows the frequency distribution of the α-tremor of the peak No.4. This is similar to the frequency distribution during the 3 years around GEJE in Fig. 7 (c). For negative α-tremor of the peak No.4, Gaussian distribution well approximates the density distribution (Fig. 8 (b2)). On the other hand, for positive α-tremor, Gaussian distribution penetrates the negative region, and does not represent positive α-tremor. The Gumbel distribution, $G(x) = exp(-exp(-x))$, fits in the positive region (Fig. 8 (b3)). The micropeaks of α-tremor in the orange dotted rectangle in fig. 8 (a) is extracted and plotted in Fig. 8 (c1). The time duration of the micropeak is 30700 sec, which is similar to the duration of the wave cluster in Fig. 3 (a). For positive α-tremor of the micropeak, Gumbel distribution well approximates the density distribution (Fig. 8 (c2)).

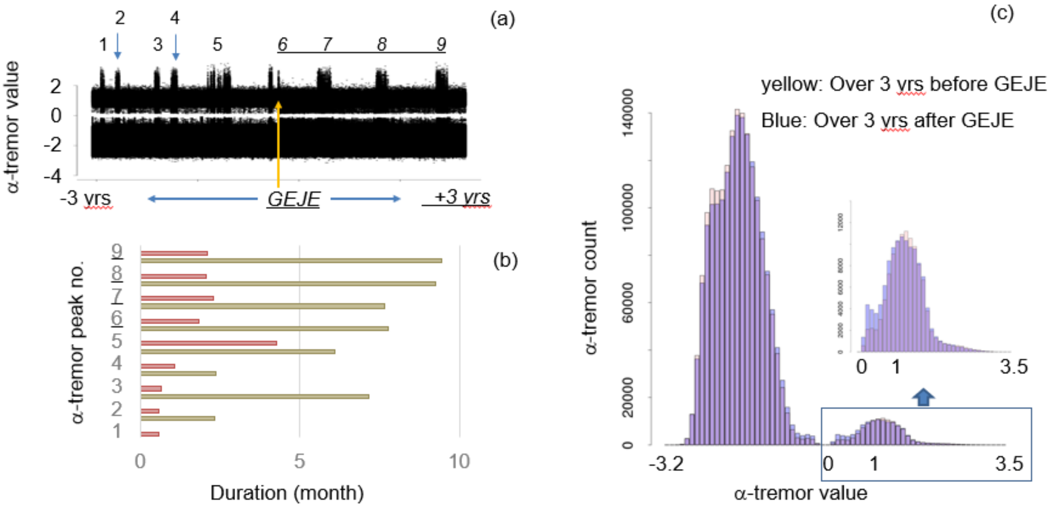

Figure 7: α-tremor at KSN over 3 years before and after GEJE. (a) The α-tremor, and the index of α-tremor peaks. (b) The time duration of the peak, and the duration of the interval between the peaks. (c) Comparison of frequency distributions of the α-tremor before and after GEJE.

Since the peaks of α-tremor in Fig.6 appear to indicate weak periodicity or seasonality, the effects of seasonal storm waves on α-tremor are investigated. Fig. 9 compares the α-tremor peaks at KSN (Figure 6) with the monthly averaged data of the hourly maximum wave height measured at Enoshima, Miyagi prefecture, the coast 64km from KSN during the period from Jan. 1, 2006 to Mar. 11, 2011. The α-tremor peaks (black) are observed at the similar timing of the wave height peaks (red). The comparison suggesting that tremors may be induced by the gravitational force generated by the waves supports the Peng and Chao's discussion that tremor occurs as a response to a driving force (Peng & Chao, 2008). Here, the location of Enoshima is indicated by the yellow filled triangle on the map in Fig. 6. The wave height data has been downloaded from the "Various data and materials: coastal wave meter observations" site of the Japan Meteorological Agency under Ministry of Land, Infrastructure, Transport and Tourism (JMA-2, 2019).

4.2 HID

Fig. 10 shows the positive α-tremor observed at HID from Jan. 1, 2009 to Dec. 30, 2018, and the timing of earthquakes with seismic intensities greater than 4. The seismic intensity was recorded at Sinhidaka Town, approximately 50km from HID. No positive α-tremor peaks are observed. The distribution of the α-tremor is uniform during the period. Only a weak positive α-tremor is observed at the timing of the earthquake B. The ground motion at HID is unaffected by the GEJE which occurred 586 km away.

The α-tremor at HID is uniform over the period (Fig. 11 (a)). The frequency distribution of the α-tremor, non-positive α-tremor, and positive α-tremor are shown in Fig. 11 (b1), 11 (b2), and 11 (b3), respectively. For both positive α-tremor and non-positive α-tremor, the Gaussian distribution is a good approximation of the frequency distribution.

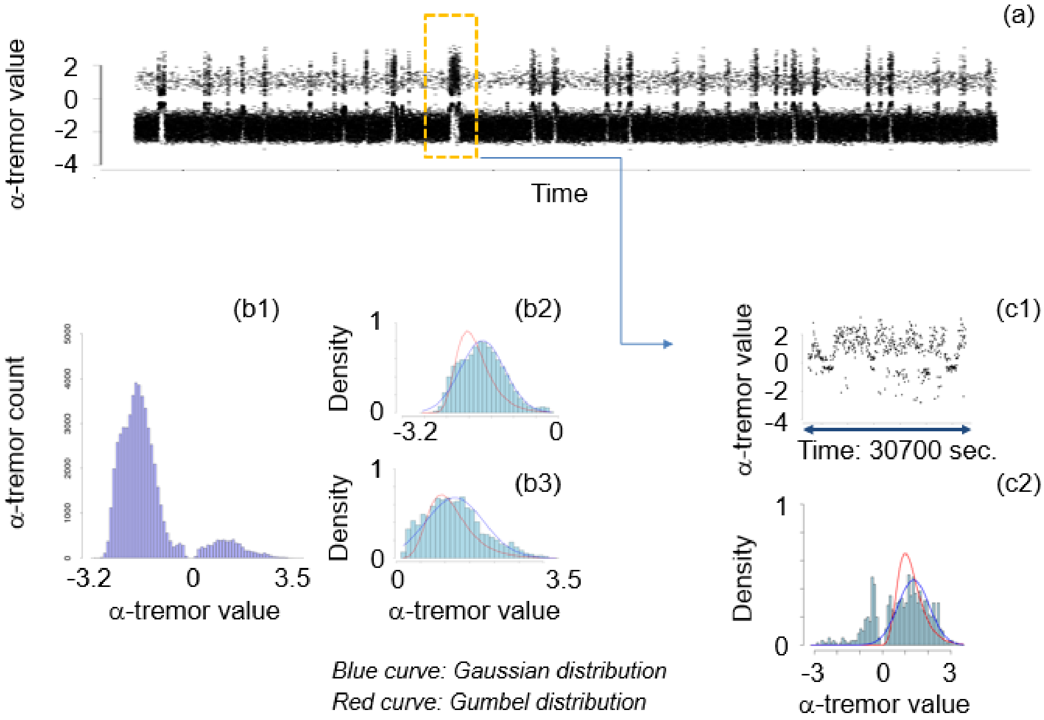

Figure 8: Fine structure of the α-tremor peak. (a) Enlarged view of the α-tremor peak No.4 in Figure 7 (a). (b1) Frequency distribution of the α-tremor peak No.4. (b2) Density distribution of the negative α-tremor of the peak No.4, and its approximations by Gaussian and Gumbel distributions. (b3) Density distribution of the positive α-tremor of the peak No.4, and its approximations by Gaussian and Gumbel distributions. (c1) The α-tremor peak extracted from the orange dotted rectangular area. (c2) Density distribution of the α-tremor in (c1), and its approximations by Gaussian and Gumbel distributions.

4.3 TMC

The seismic intensity was recorded at Kumamoto-kita Ward, approximately 39km from TMC. Fig. 12 shows the positive α-tremor observed at TMC from Jan. 1, 2008 to Jan. 10, 2019, and the timing of earthquakes with seismic intensities greater than 4. A few positive α-tremor peaks are observed before GEJE but not after GEJE. The density of the weak positive α-tremor below 1.0 is increased after GEJE.

The change in the ground motion near the GEJE timing is clearly shown in Fig. 13. The α-tremor data during the period from exactly 2.5 years before GEJE to exactly 2.5 years after GEJE are extracted (Fig. 13 (a)). The frequency distributions of the extracted α-tremor and the positive α-tremor are shown in Fig. 13 (b1) and 13 (b2), respectively. The area of the positive α-tremor distribution after GEJE is 52% of that before GEJE. The trend of the positive α-tremor after GEJE continues for about 5 years, followed by the magnitude 7.3 earthquake in April 2016. Therefore, it is suggested that the GEJE which occurred 1170 km away from TMC may have affected the ground motion at TMC, and the GEJE may have initiated the seismic process of the M7.3 earthquake.

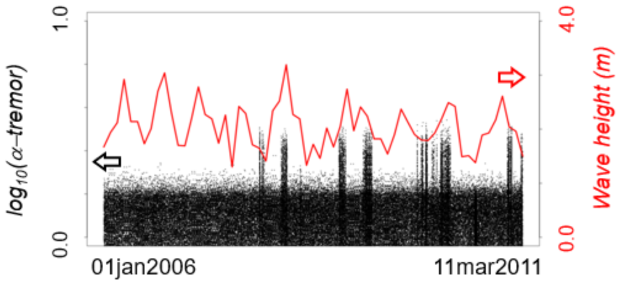

Figure 9: α-tremor at KSN and wave height on the cost near KSN.

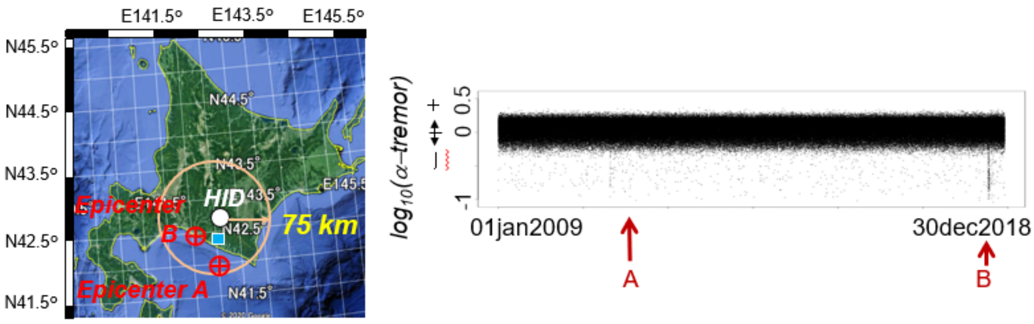

ID	Date	Magnitude	Seismic Intensity	Latitude	Longitude	Depth(km)
A	Sep. 7, 2011	5.1	5	$42.15N$	$142.35E$	10
B	Sep. 6, 2018	6.7	5	$42.41N$	$142.00E$	37

Figure 10: Positive α-tremor at HID from January 1, 2009 to December 30, 2018.

5 Conclusions

To characterize the seismic process of megathrust earthquake, we have defined α-tremor as the degree of the negative curvature of the Fourier amplitude spectrum in the frequency range of 2.97 Hz to 9.80 Hz, and evaluated the ground vibration velocity data acquired every 0.05 seconds for approximately 10 years at three seismic stations. Significant α-tremor peaks are observed only in the process of a megathrust earthquake. At the station 188 km away from the epicenter of the Great East Japan Earthquake (GEJE) of magnitude 9, symmetries regarding the seismic process of the GEJE have been found. Among the observed 9 prominent peaks of the positive α-tremor, the first and last peak appears 3 years before and after GEJE, respectively. The frequency distributions of α-tremor during the 3 years before and after the GEJE match by 99.95%. Those symmetries and the mechanism of initiating and terminating the series of the α-tremor are left for further study. The statistical distribution that properly approximates the frequency distribution of the positive α-tremor is found to be the Gumbel distribution, rather than the Gaussian distribution. The comparison of the α-tremor peak with the seasonal rise in coastal wave height suggests that α-tremor may be a mechanical response to the gravitational load generated by the waves. The time evolution of the frequency distribution of the α-tremor at the seismic station 1170 km away from the GEJE epicenter suggests

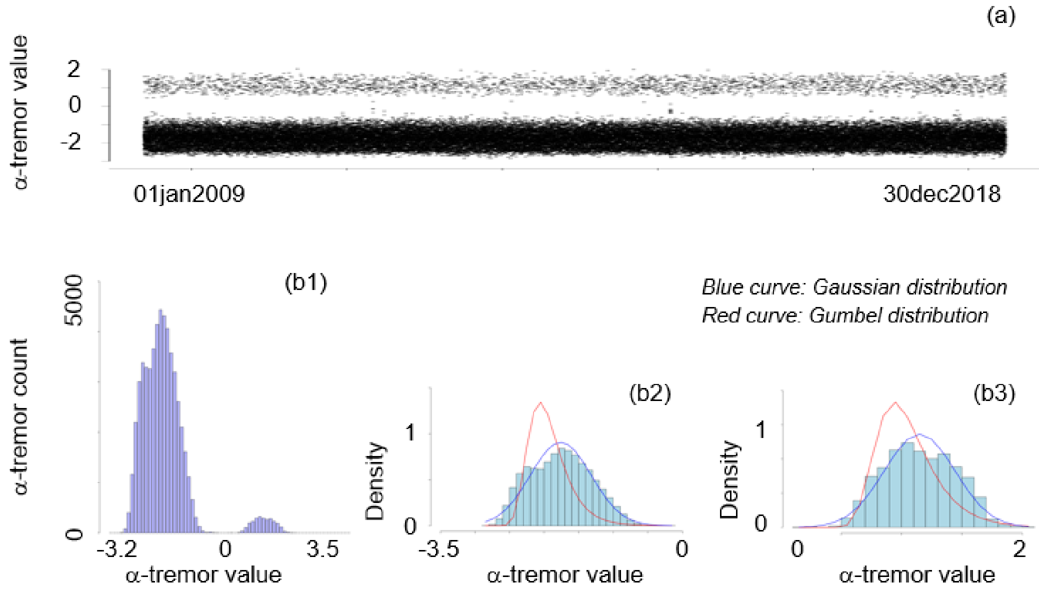

Figure 11: Frequency distribution of α-tremor at HID from January 1, 2009 to December 30, 2018. (a) α-tremor and time. (b1) Frequency distribution of α-tremor. (b2) Density distribution of negative α-tremor. (b3) Density distribution of positive α-tremor.

that the GEJE may have affected the ground motion there, and initiated the seismic process of the M7.3 earthquake that occurred near the station.

Acknowledgments

Data is publicly available through National Research Institute for Earth Science and Disaster Resilience, National Research and Development Corporation under Ministry of Education, Culture, Sports, Science and Technology. F-Net (Broadband seismograph network) data base. http://www.fnet.bosai.go.jp/top.php?LANG=en.

References

Obara, K. (2002). Nonvolcanic Deep Tremor Associated with Subduction in Southwest Japan. Science??31 May 2002: Vol. 296, Issue 5573, pp. 1679-1681. DOI: 10.1126/science.1070378

Rogers, G. & Dragert, H. (2003). Episodic Tremor and Slip on the Cascadia Subduction Zone: The Chatter of Silent Slip. Science??20 Jun 2003: Vol. 300, Issue 5627, pp. 1942-1943. DOI: 10.1126/science.1084783

Peng, Z. & Chao, K. (2008), Non-volcanic tremor beneath the Central Range in Taiwan triggered by the 2001Mw 7.8 Kunlun earthquake. Geophys. J. Int. (2008) 175, 825?829 doi: 10.1111/j.1365-246X.2008.03886.x

NIED (2019). National Research Institute for Earth Science and Disaster Resilience, National Research and Development Corporation under Ministry of Education, Culture,

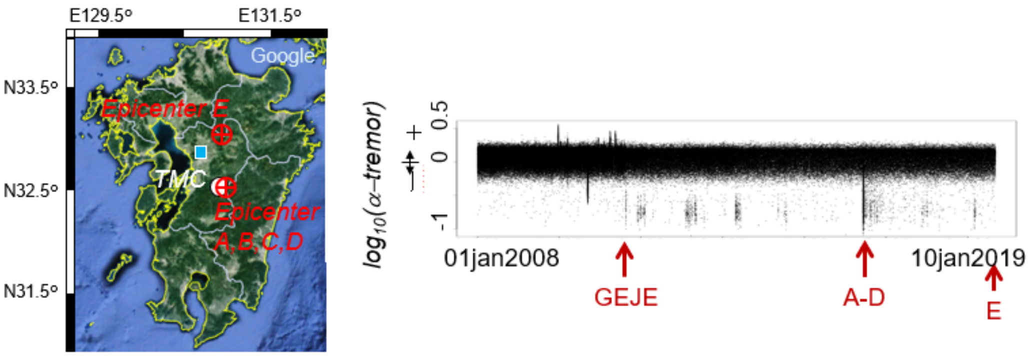

ID	Date	Magnitude	Seismic Intensity	Latitude	Longitude	Depth(km)
A	Apr. 14, 2016	6.5	5	$32.44N$	$130.48E$	11
B	Apr. 16, 2016	7.3	6	$32.45N$	$130.45E$	12
C	Apr. 16, 2016	5.4	5	$32.45N$	$130.45E$	15
D	Apr. 16, 2016	5.9	5	$32.51N$	$130.53E$	11
E	Jan. 3, 2019	5.1	5	$33.01N$	$130.33E$	10

Figure 12: Positive α-tremor at TMC from January 1, 2008 to January 10, 2019.

Sports, Science and Technology. F-Net (Broadband seismograph network) data base. DOI: 10.17598/nied.0005. http://www.fnet.bosai.go.jp/top.php?LANG=en

JMA-1. (2019). Japan Meteorological Agency under Ministry of Land, Infrastructure, Transport and Tourism. Seismic intensity database search. https://www.data.jma.go.jp/svd/eqdb/data/shindo/index.php

JMA-2. (2019). Japan Meteorological Agency under Ministry of Land, Infrastructure, Transport and Tourism. Various data and materials: Coastal wave meter observations. https://www.data.jma.go.jp/gmd/kaiyou/db/wave/obsdata/past/usw.php

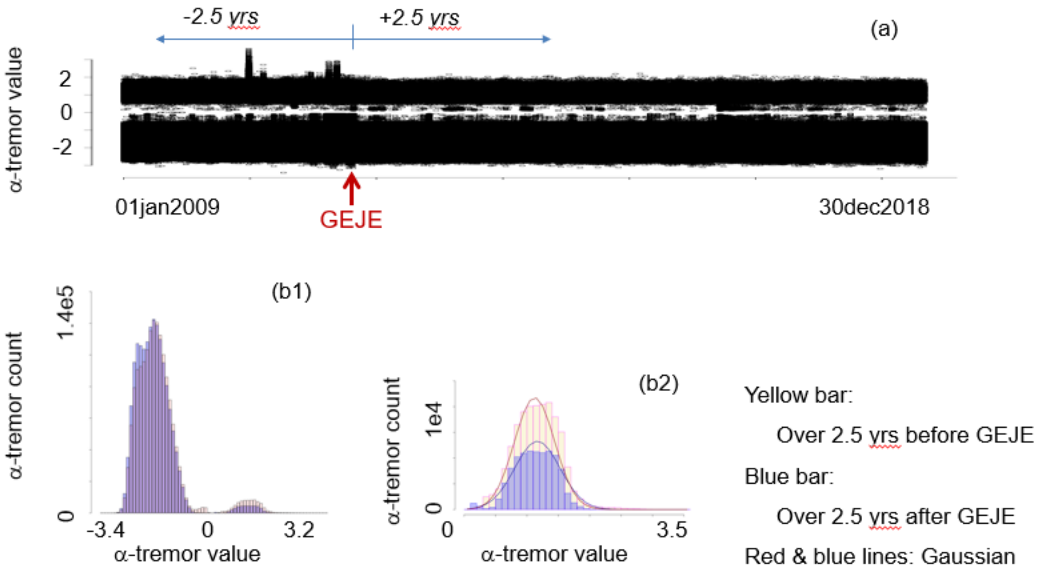

Figure 13: Frequency distribution of α-tremor at TMC over 2.5 years before and after GEJE. (a) α-tremor and time. (b1) Frequency distribution of α-tremor. Comparison before and after GEJE. (b2) Frequency distribution of positive α-tremor. Comparison before and after GEJE. Both the blue and red curves are Gaussian.